



# The escape mechanisms of the proto-atmosphere on terrestrial planets: “boil-off” escape, hydrodynamic escape and impact erosion

Ziqi Wang<sup>1</sup> · You Zhou<sup>2,3</sup> · Yun Liu<sup>1,2,3</sup>

Received: 12 September 2021 / Revised: 10 November 2021 / Accepted: 25 November 2021 / Published online: 27 January 2022  
© The Author(s), under exclusive licence to Science Press and Institute of Geochemistry, CAS and Springer-Verlag GmbH Germany, part of Springer Nature 2021

**Abstract** Atmospheric escape is an essential process that affects the evolution of the proto-atmosphere. The atmospheric escape of early terrestrial planets was extremely rapid compared with the current scenarios, and the main atmospheric escape modes were also quite different. During the dissipation of the nebula disk, the primordial atmosphere experienced a brief but violent “boiling” escape, in which most of the primordial atmosphere was lost. After the nebula disk dissipates, hydrodynamic escape and impact erosion are the two most important mass-loss mechanisms for the proto-atmosphere. Hydrodynamic escape is a rapid atmospheric escape process caused by strong solar radiation, while impact erosion refers to the process in which small-large or giant impacts erode the proto-atmosphere. In the early solar system, there were other escape mechanisms, such as non-thermodynamic escape and Jeans escape, but it is generally believed that these mechanisms have relatively little impact. Here we systematically introduce the above-mentioned atmospheric escape mechanisms and then make some suggestions for

the existing problems and future research for atmospheric escape models.

**Keywords** Proto-atmosphere · Primordial atmosphere · “Boil-off” · Hydrodynamic escape · Impact erosion

## 1 Introduction

Proto-atmosphere originated from the nebula gas disk of the young solar system. Because the protoplanets were surrounded by dense nebula gas during their growth in nebula disk, as the mass of these protoplanets increased, they would capture the surrounding nebula gas by increasing self-gravity. The captured nebula gas is a so-called primordial atmosphere (Fig. 1a), mainly consisting of hydrogen and helium (Mizuno et al. 1978; Wuchterl 1993; Ikoma et al. 2000).

Since then, the nebula disk experienced rapid dissipation, due to the material accretion towards the young Sun and evaporation caused by solar radiation such as X-ray, EUV (i.e. extreme ultraviolet), and FUV (i.e. far ultraviolet) (Gorti et al. 2015; Lammer et al. 2018). During the nebula disk dispersal, contributed by disk depressurization and more exposure to the young Sun, the primordial atmosphere experienced a short but violent atmospheric escape. Owen and Wu (2016) named this process a “boil-off” (Fig. 1b). They suggested that after the end of “boil-off”, around 90% of the initial primordial atmospheric mass might have been lost. The Earth and Mars might lose their primordial atmospheres completely, whereas Venus might capture a tiny primordial atmosphere after disk dispersal (Erkaev et al. 2014; Stökl et al. 2016; Odert et al. 2018; Lammer et al. 2018).

✉ You Zhou  
zhouyou06@cdu.cn

✉ Yun Liu  
liuyun@vip.gyig.ac.cn

<sup>1</sup> State Key Laboratory of Ore Deposit Geochemistry, Institute of Geochemistry, Chinese Academy of Sciences, Guiyang 550081, China

<sup>2</sup> International Research Center for Planetary Science, College of Earth Sciences, Chengdu University of Technology, Chengdu 610059, China

<sup>3</sup> CAS Center for Excellence in Comparative Planetology, Hefei 230026, China

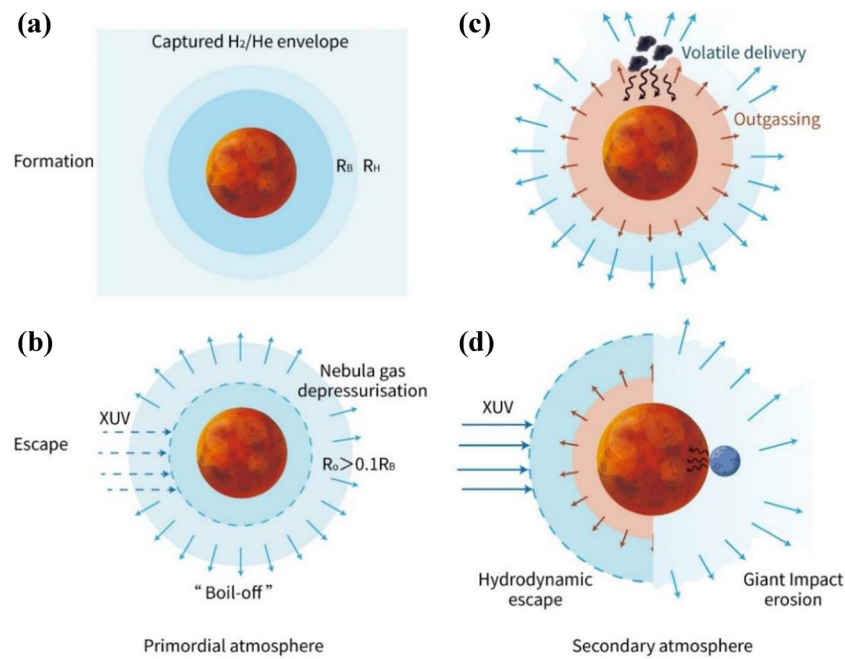


**Fig. 1** Illustration of formation and escape of proto-atmosphere for terrestrial planets, **a, b** for the primordial atmospheres, **c, d** for the secondary atmospheres. **a** Illustrates that when growing protoplanets were embedded in nebula disk, this outer boundary of proto-atmosphere can be estimated by Hill radius and Bondi radius. Hill radius is often simplified as the boundary where the gravity of the planet balances the tidal force from the Sun (Lammer et al. 2014; Massol et al. 2016). Bondi radius is the boundary where the thermal motion of gas molecules will dominate the protoplanet's gravity, within it the gases move towards a freefall solution (Edgar 2004). The planetary outer boundary is defined as the minimum of  $R_H$  and  $R_B$

The impact events during the accretion process of protoplanets contributed more material sources to proto-atmosphere. The giant impacts led to the formation of global magma oceans. During the solidification of these magma oceans, a great amount of volatiles would be catastrophically outgassed from the mantle to the atmosphere (Fig. 1c). For small-large impacts, a large amount of volatiles could be retained in the proto-atmosphere as the impactors traveled through the proto-atmosphere. Generally, after the outgassing and volatile delivery caused by the impact process, a protoplanet could build up a dense steam atmosphere mainly composed of  $H_2O$  and  $CO_2$ , namely secondary atmosphere (Elkins-Tanton 2008, 2011; Marcq 2012; Hamano et al. 2013; Lebrun et al. 2013; Massol et al. 2016; Salvador et al. 2017). The primordial atmosphere and the secondary atmosphere together constitute the proto-atmosphere.

Obviously, the major atmospheric escape mechanism for proto-atmosphere is quite different from that for the present atmosphere, and the atmospheric mass-loss process corresponding to the former could be much more efficient. After the short “boil-off”, there are two remarkable atmospheric escape mechanisms for proto-atmosphere: hydrodynamic escape and impact erosion (Fig. 1d). Without the shield of nebula gas, the primordial atmosphere would be exposed to the high flux of solar XUV (X-ray and

EUV). Hydrodynamic escape, driven by atmospheric absorption of XUV from the young Sun, can be extremely efficient on a global scale especially when the main component of the upper atmosphere is hydrogen. A large amount of volatiles can be lost due to hydrodynamic escape (Odert et al. 2018; Tian et al. 2018; Benedikt et al. 2020; Lammer et al. 2020). Impact erosion mechanism can be divided into two regimes, depending on the impact energy of impact events: small-large impacts induce local atmospheric escape, while giant impacts can produce a strong shock traveling through the whole planet and thus induce a global atmospheric escape (Chen and Ahrens 1997; Schlichting et al. 2015; Schlichting and Mukhopadhyay 2018).

## 2 Basic conceptions of atmospheric escape

Atmospheric escape mainly happens in the upper atmosphere. The planetary upper atmosphere is an essential part of atmospheric escape models. It can be defined as a “heterosphere” (i.e. a region where the different atmospheric species begin to separate from each other due to planetary gravity and the weak mixing). It can also be identical to the “thermosphere”, which can be heated efficiently by the absorption of solar XUV. Since the lower boundary of the heterosphere is normally located not far

from that of the thermosphere, the lower boundaries in most atmospheric escape models do not strictly distinguish between the base of the heterosphere and thermosphere.

The height at which collisions among atmospheric particles cease to be important is called the critical level. The atmosphere above this critical level is called the exosphere (Spitzer 1952), or planetary corona by Chamberlain (1963). Therefore, this critical level can be called as exobase, regarded as a surface or a narrow atmospheric region.

Jeans escape is a classical atmospheric escape process. It assumes that the atmosphere near the exobase is in hydrostatic equilibrium, and the particles near the exobase have a Maxwell velocity distribution. The high energy tail of this Maxwell distribution directly leads to a molecule-by-molecule atmospheric escape, named Jeans escape (Chamberlain 1963). It can be calculated as:

$$\Phi = \frac{n(z)V_0}{2\sqrt{\pi}} \left( \frac{V_{esc}^2}{V_0^2} + 1 \right) \exp\left(-\frac{V_{esc}^2}{V_0^2}\right) \quad (1)$$

here  $\Phi$  is the Jeans escape flux (number of escaping particles per unit area per unit time) at the exobase,  $n(z)$  is the local number density of particles,  $V_0$  is the most probable velocity related to the local atmospheric temperature,  $V_{esc}$  is the escape velocity.

Jeans escape happens in atmospheres that are not superheated by solar radiation in scenarios such as these in the present solar system. However, the scenario could be quite different much earlier. Opposite to the increasing luminosity of the Sun, the solar EUV decreases as the Sun evolves (Ribas et al. 2005; Johnstone et al. 2015; Tu et al. 2015), for which EUV flux from the young Sun can be much higher than the present. Under several tens to hundreds of times higher solar EUV flux, the upper atmosphere can be heated up efficiently, leading to a shifted Maxwell distribution (Yelle 2004). In this case, the hydrodynamic escape instead of Jeans escape occurs. Traditionally, hydrodynamic escape with an extremely high mass-loss rate can also be called a “blow-off”. It can be considered as a global atmospheric expansion like a cometary tail, during which the bulk of upper atmospheric particles escape rapidly.

However, in a much earlier period, back to the point when the nebula disk dissipated, there could be once another mechanism called “boil-off”, which could be much more violent than hydrodynamic “blow-off”. “Boil-off” can be considered as a strengthened “blow-off”. It refers to a process that a proto-atmosphere not only experiences a fast escape like hydrodynamic “blow-off” induced by solar EUV, but also contributed by the depressurization of the surrounding nebula gas, which further leads to a much more violent atmospheric escape. According to the sequence of these remarkable

atmospheric escape processes, here we introduce the “boil-off” first, then the hydrodynamic escape and impact erosion.

### 3 The “boil-off”

Ikoma and Hori (2012) first investigated the effect of depressurization on atmospheric escape during the dispersal of nebula disks. They thought this depressurization caused by nebula disk dispersal could lead to a special atmospheric escape mechanism. They also examined the preservation of primordial atmosphere on super-Earths. Owen and Wu (2016) further investigated this process and named it “boil-off”, and suggested that the disk depressurization could lead to a violent atmospheric escape during “boil-off”. According to the “boil-off” theory, when the disk dissipates, there are two processes allowing the primordial atmosphere to expand and then undergo an efficient escape: (a) the disk dissipation lead to depressurization of surrounding proto-atmosphere and gravitational contraction of the protoplanet; (b) as the protection of the nebula gas decreases, the upper primordial atmosphere is heated up due to direct exposure to the XUV radiation of the young Sun (Owen and Wu 2016; Fossati et al. 2017). Owen and Wu (2016) suggested that how fast the disk dissipation happens might have an essential influence on “boil-off”. If disk pressure drops too slowly then the “boil-off” could be less important. Kubyskhina et al. (2018) suggested that the mass of planets might also have an essential effect on “boil-off”. During the “boil-off”, the highest mass-loss rates correspond to the lowest gravity planets, and the dependence of the mass-loss rates on the stellar XUV flux tends to get strengthened with increasing planetary mass.

The primordial atmosphere experiences “boil-off” until the outer boundary has contracted to  $0.1R_B$  (Owen and Wu 2016), lasting from 0.1 up to a few Ma (Lammer et al. 2020). Thereafter the main atmospheric escape mechanism transfers from “boil-off” to XUV-driven hydrodynamic escape.

The planetary outer boundary is defined as the minimum of  $R_H$  and  $R_B$ , generalized for most cases  $R_B$  with  $R_B < R_H$  (Ikoma and Genda 2006; Lammer et al. 2014), and therefore the boundary of primordial atmosphere is often placed at the Bondi radius  $R_B$ . The Bondi radius  $R_B$  can be calculated as:

$$R_B = \frac{GM_{pl}}{2c_s^2} \quad (2)$$

where  $G$  is the gravitational constant,  $M_{pl}$  is the mass of the planet,  $c_s$  is the isothermal sound speed of the surrounding gas.

## 4 Hydrodynamic escape

After the “boil-off”, the upper proto-atmosphere continues to be heated efficiently by the intensive irradiation of XUV from the young Sun. Hydrodynamic escape is a global, cometary-like, expansion of the atmosphere with an extremely high mass-loss rate. This process can also be called a “blow-off” or planetary wind. It can be significant especially for an H-rich atmosphere, in which atomic hydrogen, as the dominant atmospheric escape particles, can drag other heavier species away from the planet (Fig. 2). Therefore, the mass-loss rates of heavy components like CO<sub>2</sub> and noble gases increase during a hydrodynamic escape.

### 4.1 The structure of planetary upper atmosphere

Tian et al. (2008) calculated the temperature profiles of the thermosphere under different solar EUV fluxes. The peak temperature in the thermosphere occurs at the exobase level for solar EUV fluxes smaller than about 5 EUV (5 times that of today). However, for EUV flux values greater than about 5 EUV, the upper part of the thermosphere begins to get cooler. In this case, Tian et al. (2008) concluded that the higher energy input into the thermosphere, the lower the exobase temperature would be in hydrodynamic atmospheres, which is consistent with previous works (Watson et al. 1981; Kasting and Pollack 1983; Chassefière 1996; Yelle 2004; Tian et al. 2005).

### 4.2 The development of hydrodynamic escape theory

Parker (1964) proposed the hydrodynamic escape theory to study the solar wind plasma and found that the solar mass

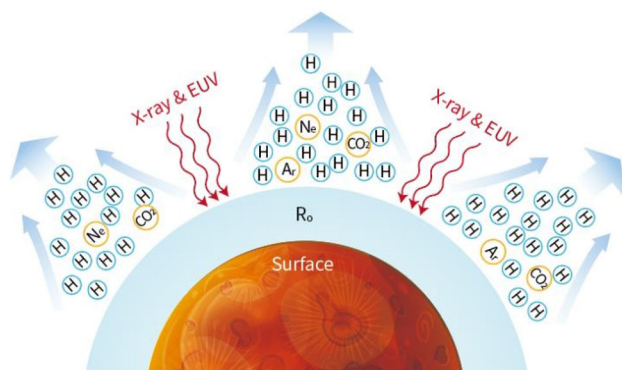


**Fig. 2** Illustration of heavy particles dragged by hydrogen atoms in hydrodynamic flows. Heavy particles (like Ne, Ar, CO<sub>2</sub>) can be dragged along the atomic hydrogen to space due to the much higher escape flux of the latter. Moreover, some of the heavy particles that escape in a high enough flux can put force on heavier ones as well

loss process is caused by the expansion of the outer part of the Sun. This expansion is determined by the exosphere temperature, ranging from the exobase to the altitude above which the atmospheric escape flow becomes supersonic (traditionally a rapid atmospheric escape is described as a gas that goes sonic, especially for hydrodynamic escape). Watson et al. (1981) first applied the hydrodynamic escape theory to study the escape process of H-rich proto-atmospheres from the Earth and Venus, since they suggested that the hydrodynamic escape of a light gas from a planetary atmosphere is a process similar in many respects to the supersonic flow of plasma from the Sun. Watson et al. (1981) also first defined energy-limited atmospheric escape and suggested that the atmospheric escape rate should have been controlled by heating from solar EUV. Kasting and Pollack (1983) investigated the hydrodynamic escape process on early Venus. They suggested that the time required for Venus to have lost the bulk of a terrestrial ocean of water is on the order of a billion years. Kasting and Pollack (1983) assumed a value of stellar EUV radiation close to the present Sun, while Ribas et al. (2005) pointed out that the young Sun’s EUV flux could be several tens to hundreds of times higher than the present solar value.

Tian et al. (2005) pointed out that the Archean Earth was surrounded by a H-rich atmosphere with a cold exobase. In such a condition they suggested that energy-limited EUV-driven hydrodynamic escape of hydrogen molecules should have been the dominant atmospheric escape mechanism. Tian et al. (2005) established a hydrodynamic escape model with 1D time-dependent non-viscous Euler equations, they took a constant 250 K as the lower boundary temperature, lack of detailed calculations on radiative transfer processes in the lower part of the atmosphere. Catling (2006) argued that Tian et al. (2005) neglected the importance of the nonthermal escape mechanism. Tian et al. (2006) responded that the nonthermal escape rate of early Earth in Archean can only be lower than that of early Venus, which cannot balance the volcanic volatile outgassing rate, making it necessary for the early Earth to experience a rapid hydrodynamic escape.

For early Earth with the same composition as that of today, Kulikov et al. (2007) established a model, predicting a thermospheric temperature of 10,000 K for EUV fluxes about 12 times that of the present. The extremely high thermospheric temperatures of Kulikov et al. (2007) showed that the thermosphere cannot be considered hydrostatic in extreme solar EUV conditions because atomic oxygen (the dominant gas in the upper thermosphere of the present Earth) should be escaping at a significant rate.

Erkaev et al. (2015) applied a 1-D hydrodynamic upper atmosphere model to study the XUV-driven thermal escape

of the martian proto-atmosphere during the early active stage of the young Sun. They set a solar XUV flux that is 100 times higher than the present value. Depending on the amount of the outgassed volatiles, as well as the assumed heating efficiency and location of the lower thermosphere, their results indicated that early Mars lost its nebular captured hydrogen envelope and catastrophically outgassed steam atmosphere most likely within 0.4–12 Ma by hydrodynamic escape.

Lammer et al. (2014) assumed an EUV radiation value which is 100 times higher than the present value. They investigated the escape process of the primordial atmosphere on protoplanets ranging from 0.1 to 5  $M_{\text{Earth}}$ . The results suggested that for protoplanets with mass  $< 1 M_{\text{Earth}}$  the primordial atmosphere could be lost within 500 Ma. They suggested that solar system terrestrial planets may lose their nebula-based proto-atmospheres during the XUV activity saturation phase of the young Sun.

### 4.3 Hydrodynamic escape model for hydrogen-dominated atmosphere

Numerical models related to hydrodynamic escape are generally based on the energy-limited theory (Watson et al. 1981; Erkaev et al. 2007, 2013, 2014; Luger et al. 2015; Ginzburg et al. 2016; Odert et al. 2018; Benedikt et al. 2020; Lammer et al. 2020). The energy-limited theory basically assumes that the total atmospheric mass-loss rate is limited by the solar radiation energy heating up the thermosphere, which fits the scenarios of hydrodynamic escape for hydrogen-dominated atmosphere well. The  $\text{H}_2\text{O}$  molecules in the upper atmosphere on early terrestrial planets can be dissociated after absorbing stellar XUV radiation, and thus hydrogen atoms become the dominant particles from the base of thermosphere to the Roche lobe boundary (Kasting and Pollack 1983; Chassefière 1996; Yelle 2004; Koskinen et al. 2010; Lammer et al. 2013). As the upper atmosphere temperature reaches about 2000 K, the  $\text{H}_2$  molecules break down thermally into hydrogen atoms (Lammer 2012). This hydrogen-dominated upper atmosphere can then absorb stellar XUV radiation effectively, which makes XUV radiation a controlling factor during a hydrodynamic escape. In this case, if the efficiency of heating in the thermosphere remains unchanged, no matter how fast atmospheric escape can be at the exobase level, total escape remains unchanged. Thus the calculations of atmospheric escape and the evolution history of planetary atmospheres with strongly heated thermosphere can be simplified (Tian 2013).

Erkaev et al. (2007) developed an energy-limited equation to estimate the total mass-loss rate from a “hot Jupiter”:

$$M = \frac{\pi r_{\text{XUV}}^2 I_{\text{Sun}}}{\Phi_0 K (r_{\text{Rl}}/r_{\text{pl}})} \quad (3)$$

where  $M$  refers to the total mass-loss rate, and it equals the ratio between the stellar XUV radiation absorbed by the atmosphere and a gravitational potential variation.  $\Phi_0 K (r_{\text{pl}}/r_{\text{pl}})$  refers to the gravitational potential difference between the Roche lobe boundary ( $r_{\text{Rl}}$ ) and the planetary surface ( $r_{\text{pl}}$ ) affected by solar tidal forces.  $I_{\text{Sun}}$  equals to the solar XUV flux, and  $r_{\text{XUV}}$  equals the distance from the Sun to the planet.

Owen and Jackson (2012) found that at orbits  $> 0.1$  AU, heating by EUV photons becomes the dominant driver for hydrogen escape in the hydrodynamic regime. Odert et al. (2018) calculated the escape of three-component secondary atmosphere on Mars-sized protoplanets with a simplified Eq. (3). They transferred it into:

$$M = \frac{\beta^2 \eta F_{\text{EUV}}}{4\Delta\Phi} = m_{\text{H}} F_{\text{H}} + m_{\text{O}} F_{\text{O}} + m_{\text{CO}_2} F_{\text{CO}_2} \quad (4)$$

Benedikt et al. (2020) then expanded Eq. (4) to a multi-species atmosphere:

$$M = \frac{\beta^2 \eta F_{\text{EUV}}}{4\Delta\Phi} = m_{\text{H}} F_{\text{H}} + \sum_{i=1}^n m_i F_i \quad (5)$$

where  $\beta$  is the ratio of the radius where the bulk of the incoming EUV radiation is absorbed ( $R_0$ ) to the planet radius ( $r_{\text{pl}}$ ), and it is often taken as 1;  $\Delta\Phi$  is the gravitational potential at the surface of the planet,  $F_i$  is the escape flux of species  $i$  in  $\text{cm}^{-2} \text{s}^{-1}$ , and  $\eta$  is the non-dimensional solar heating efficiency. Murray-Clay et al. (2009) suggested that  $\eta$  should be less than 20% for EUV heating during the first 100 Ma of the solar age. Several other research groups took  $\eta$  as 15% (Erkaev et al. 2007, 2014; Penz et al. 2008; Odert et al. 2018; Benedikt et al. 2020).

Hydrogen atoms can drag along other heavier particles like oxygen and noble gases to space during its hydrodynamic escape. According to Zahnle and Kasting (1986) and Zahnle et al. (1990), the escape flux of the dragged heavy species  $i$  ( $F_i$ ) can be described as

$$F_i = F_{\text{H}} f_i x_i \quad (6)$$

where  $f_i$  is the mixing ratio relative to atomic hydrogen and  $x_i$  is the fractionation factor equals the velocity ratio  $v_i/v_{\text{H}}$ .

Combining Eq. (5) with (6) allows expressing the escape flux of the atomic hydrogen as:

$$F_{\text{H}} = \frac{\beta^2 \eta F_{\text{EUV}}}{4\Delta\Phi (m_{\text{H}} + \sum_{i=1}^n m_i f_i x_i)} \quad (7)$$

According to Zahnle et al. (1990), the fractionation factors of oxygen atoms ( $x_{\text{O}}$ ) and other heavy species ( $x_i$ ) can be written as:

$$x_O = 1 - \frac{g(m_O - m_H)b_{H,O}}{F_H k_B T (1 + F_O)} \quad (8)$$

$$x_i = \frac{1 - \frac{g(m_i - m_H)b_{H,i}}{F_H k_B T} + \frac{b_{H,i}}{b_{H,O}} f_O (1 - x_O) + \frac{b_{H,i}}{b_{O,i}} f_O x_O}{1 + \frac{b_{H,i}}{b_{O,i}} f_O} \quad (9)$$

where  $g$  refers to the gravitational acceleration at the base of the escaping flow, like 1  $\mu$ bar level in Benedikt et al. (2020).  $m$  is the mass of the individual particle.  $b$  is the binary diffusion coefficients.  $k_B$  is the Boltzmann constant and  $T$  is the temperature of the upper atmosphere.

Then one can combine Eqs. (6) to (9) to calculate the hydrodynamic escape process of a secondary atmosphere. Moreover, a hydrogen envelope with a moderate mass around early Earth may have acted as a shield against atmosphere erosion by the solar wind plasma during the first hundred Ma (Kislyakova et al. 2013) and could have thus protected heavier species, such as  $N_2$  molecules, against rapid atmospheric loss (Lichtenegger et al. 2010; Lammer et al. 2013). It should be noted that hydrodynamic escape has been existing during the “boil-off” phase, mainly driven by continuum stellar radiation, while the “boil-off” is powered by the binding energy released during the rapid gravitational contraction (Owen and Wu 2016), leading to the escape rates of “boil-off” orders of magnitude higher than those resulting from the EUV-driven hydrodynamic escape (Odert et al. 2018).

#### 4.4 The transition from hydrodynamic escape to Jeans escape

Jeans escape parameter  $\lambda$  is often used to evaluate when the hydrodynamic escape terminates and starts transferring to Jeans escape. It represents the ratio of the gravitational to the thermal energy of the atmospheric molecules:

$$\lambda = \frac{GMm}{rkT} \quad (10)$$

where,  $G$  is Newton’s gravitational constant.  $M$  is the planetary mass.  $m$  is the mass of the atmospheric main species.  $k$  is Boltzmann constant.  $r$  is the distance from the center to the altitude of the molecules in a specific question and  $T$  is the corresponding atmospheric temperature.

The transition from Jeans escape to hydrodynamic escape can be considered to start in scenarios for  $\lambda < \lambda_0$ . As is shown in Table 1, there is a series of values of  $\lambda_0$  taken by different groups, varying from 1 to 3. These differences can be considered as in a small range. They should be induced by different boundary conditions and solution treatments of the models.

During the transition from hydrodynamic escape to Jeans escape, the upper atmosphere would not transfer into hydrostatic equilibrium immediately. As the EUV flux

decreases, there is a stage that the thermosphere still remains in dynamical expansion meanwhile the atmospheric escaping flow does not reach the escape velocity at the exobase level. In this stage, the upper atmosphere remains in a hydrodynamic regime but actually experiences a fast Jeans escape (Tian et al. 2008).

The lasting time of the hydrodynamic escape with extreme mass-loss rates depends generally on the evolving solar EUV flux, the planetary gravity, and orbit location, the main constituents in the upper part of proto-atmosphere. The hydrodynamic escape would eventually transfer to Jeans escape. However, for a better understanding of this transition timescale on early Venus, Earth and Mars, it is crucial to gain a clearer knowledge of the early evolution of the Sun, especially of its EUV flux during the first 1 Ga.

#### 4.5 The difference among Jeans escape, hydrodynamic regime, and hydrodynamic escape

The distinction between Jeans escape and hydrodynamic escape is analogous to that between evaporation and boiling. In this analogy, the exobase, the force of gravity, and the collision binding of other molecules can be separately compared to the surface of the evaporating fluid, the atmospheric pressure, and the pressure of other molecules in the liquid. Moreover, Jeans escape does not change the temperature and the velocity distributions of particles in the upper atmosphere, while the hydrodynamic escape does modify both two states through its significant effect on the atmospheric energy budget.

Jeans escape mainly happens in a “collisionless” region above the exobase, where the velocities of partial neutral species could exceed the escape velocity of the planet. Below the exobase, the frequent collision among atmospheric particles and planetary gravity prevents the atmosphere from escaping. Once the atmosphere was heated efficiently, especially in the early solar system, the atmosphere would be in a hydrodynamic regime. In the hydrodynamic regime, the particles become so energetic that the collisions become insufficient to restrict escape. Thus, the hydrodynamic escape can take place far below the exobase. The lower boundary of a hydrodynamic escape model is commonly set around the base of thermosphere.

It should be noted that a planetary atmosphere in the hydrodynamic regime does not have to experience hydrodynamic escape. The former can be considered as a necessary but not sufficient condition to the latter. The hydrodynamic regime can be reached when the atmospheric escape flow becomes important to affect the atmospheric energy budget, while the hydrodynamic escape occurs when the heating of the upper atmosphere is

**Table 1** Values of  $\lambda_0$  taken by different authors

Authors	$\lambda_0$
Öpik (1963), Tian et al. (2008), Lammer et al. (2008), Lammer (2012)	1.5
Hunten (1982), Young et al. (2019)	2
Johnson et al. (2013)	Monatomic gases 2.1
	Diatomic gases 2.8–3.5
Gronoff et al. (2020)	Monatomic gases 1.5
	Diatomic gases 2.5

so strong that the bulk kinetic energy of the upper atmosphere particles overcome the planetary gravity, leading to a significant effect on the energy budget.

## 5 Impact-induced atmospheric erosion

Impact-induced atmospheric erosion is another essential mechanism controlling atmospheric escape. Many studies indicate that the impact events were in a high frequency in the earliest stage of planet formation (Gomes et al. 2005; Morbidelli et al. 2018; Xie et al. 2021). Depending on the energy released from the impact events, the impact events can be divided into three regimes: small impacts, large impacts, and giant impacts.

Figure 3 shows simplified impact patterns of the three impact regimes. The small impacts partially eject the atmosphere beyond the tangent plane of the impact site, and the ejected atmosphere shapes in a cone centering at the impact site (Fig. 3a). The more energy released from the impactor, the more atmosphere will be ejected, which corresponds to a larger angle  $\theta$  of the cone. A large impact occurs when  $\theta$  increases to  $\pi/2$ , thus the whole atmosphere above the tangent plane will be lost (Fig. 3b), meanwhile, the energy released from the impactor is yet not able to cause a global earthquake. The ratio of the atmospheric mass above the tangent to the total atmospheric mass

equals  $h/2R$  ( $h$  is the atmospheric scale height and  $R$  is the planetary radius) (Schlichting et al. 2015; Schlichting and Mukhopadhyay 2018). Giant impacts lead to a global escape of the atmosphere as the impactor has enough high kinetic energy (Fig. 3c). In this scenario, a global earthquake occurs and the energy released from the impact will not only eject the whole atmosphere above the tangent plane of the impact site but also produce shock waves spreading through the whole planet and then delivering energy from the ground to the atmosphere. In this case, a global-scale atmospheric escape occurs.

The net atmospheric loss caused by the impact events mainly depends on three factors: (1) the size distribution of the impactors (reflecting the possible intensity of the collision denudation process); (2) volatile content of impactor; (3) the formation and outgassing process of magma oceans caused by impact events. Early models (Melosh and Vickery 1989) regarded the atmospheric density around the impact point as isotropic. However, the atmospheric column density increases significantly in the direction close to the tangent plane (Schlichting et al. 2015). Therefore, column density above the impact site is the lowest, and oppositely the density along the tangent plane is the highest, corresponding to the simplest and most difficult atmospheric erosion process.

### 5.1 Impact erosion model for small-large impacts

Analytical models of small-large impacts are often based on the calculation method developed by Zel'dovich and Raizer (1967). Only a few groups investigated the low-speed impact events participated by planetesimals (Melosh and Vickery 1989; Vickery and Melosh 1990; Ahrens 1993; Schlichting et al. 2015). The mass of the ejected atmosphere in small-large impacts can be calculated by Eq. (11) (Schlichting et al. 2015):

$$M_{Eject,\theta} = 2\pi\rho_0 \int_{a=0}^{a=\infty} \int_{\theta'=0}^{\theta'= \theta} \exp[-z/h] \sin \theta' a^2 d\theta' da \quad (11)$$

where  $\rho_0$  is the atmospheric density on the ground,  $a$  is the distance from the impact site to the top of the atmosphere,  $\theta$  is the solid angle centered at the impact site,  $z$  is the

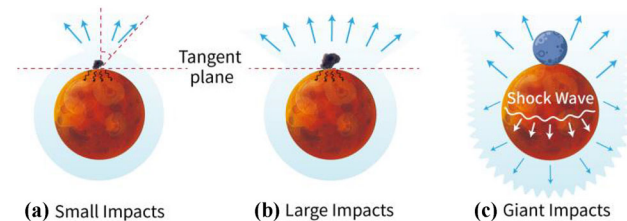


**Fig. 3** Illustration of the small impacts, large impacts, and giant impacts. **a** Small impacts: the low-kinetic impactors such as low-mass planetesimals can only eject limited local atmosphere shaping in a cone within  $\theta$ . **b** Large impacts: the low-kinetic impactors can erode the whole atmosphere above the tangent plane of the impact site. **c** Giant impacts: the shock waves produced by high-energy impactors spread from the impact site to the whole planetary surface, causing a global atmospheric escape

height in the atmosphere measured from the ground, and  $h$  is the atmospheric scale height.

Assuming that the density and velocity of an impactor are constant. At first, with the increase of the impactor size, the corresponding ejection cone of the equivalent explosion scope gets larger (corresponding to larger  $\theta$ ). Then due to the harder erosion process in a larger cone, the ratio of ejected atmospheric mass to impactor mass  $M_{Eject}/m_{Imp}$  (corresponding to the erosion efficiency) will peak and soon decrease (Schlichting et al. 2015). As the size of the impactor gets large enough to eject all the atmosphere on the tangent plane of the impact point (i.e. large impact) but not as large as that of the giant impact, the erosion efficiency will further get reduced. Moreover, considering a proto-atmosphere without supply, the later small-large impacts occur, the higher atmospheric erosion efficiency will be.

## 5.2 Giant impact events

Chen and Ahrens (1997) developed the first numerical model on atmospheric impact erosion. They suggested the energy released from a giant impact could induce a strong ground motion around the whole planetary surface, accelerating the atmosphere to escape, based on this they developed a one-dimensional atmosphere escape model. Genda and Abe recalculated the ground velocity by SPH method and modified the atmospheric mass-loss induced by giant impacts, based on a one-dimension hydrodynamic model described as:

$$\frac{D\tilde{r}}{D\tilde{t}} = \frac{1}{4\pi\tilde{r}^2\tilde{\rho}} \quad (12)$$

$$\frac{D\tilde{u}}{D\tilde{t}} = -\frac{4\pi\tilde{r}^2}{\gamma} \frac{\partial\tilde{\rho}}{\partial\tilde{m}} - \frac{\lambda_0}{\gamma\tilde{r}^2} \quad (13)$$

$$\frac{D\tilde{r}}{D\tilde{t}} = \tilde{u} \quad (14)$$

$$\frac{D\tilde{p}}{D\tilde{t}} = -4\pi\gamma\tilde{\rho}\tilde{p} \frac{\partial\tilde{r}^2\tilde{u}}{\partial\tilde{m}} \quad (15)$$

where  $\gamma$  is the adiabatic index,  $r$  is the path the particles travel through and  $\tilde{u}$  is the corresponding speed,  $m$  is the atmospheric particle mass.  $\tilde{\rho}$  and  $\tilde{p}$  are the local number density and temperature, respectively.

Equations (12) and (13) describe the atmospheric motion related to the global ground shock given by the Lagrangian equations. Equation (15) expresses the energy equation of an adiabatic gas. The results suggested that the globally averaged ground velocity is smaller than 6 km/s, thus up to 30% of the atmosphere escapes during a giant impact (Genda and Abe 2003, 2005).

Schlichting et al. (2015) developed a new one-dimension model to calculate the ground velocity and

atmospheric mass-loss rate during a giant impact. They established empirical equations of atmospheric erosion induced by giant impacts. Assuming momentum conservation and a constant density impacted the planet, the velocity of the shock wave spreading through the planet  $v_s$  and the ground velocity  $v_g$  by which the energy transfer to the atmosphere from the solid surface can be calculated from Eqs. (16) and (17) respectively.

$$v_s = v_{imp} \left(\frac{m}{M}\right) \frac{1}{(l/2R)^3(4 - 3(l/2R))} \quad (16)$$

$$v_g = v_{imp} \left(\frac{m}{M}\right) \frac{1}{(l/2R)^2(4 - 3(l/2R))} \quad (17)$$

where  $v_{Imp}$  is the velocity of the impactor,  $l$  is the distance of the shock wave traveling from the impact site,  $m$  is the mass of the impactor.  $M$  and  $R$  are the mass and radius of the planet, respectively.

Isothermal atmosphere and adiabatic atmosphere are often used as the critical conditions for calculation since the physical and chemical conditions of the early atmosphere are full of uncertainty. The atmospheric loss fraction  $X_{loss}$  is a function when  $(v_{Imp}/v_{esc})(m/M) \ll 1$ . Equations (18) and (19) are the global atmospheric loss rate under isothermal and adiabatic atmosphere respectively:

$$X_{loss} = 0.4 \left(\frac{v_{Imp}m}{v_{esc}M}\right) + 1.4 \left(\frac{v_{Imp}m}{v_{esc}M}\right)^2 - 0.8 \left(\frac{v_{Imp}m}{v_{esc}M}\right)^3 \quad (18)$$

$$X_{loss} = 0.4 \left(\frac{v_{Imp}m}{v_{esc}M}\right) + 1.8 \left(\frac{v_{Imp}m}{v_{esc}M}\right)^2 - 1.2 \left(\frac{v_{Imp}m}{v_{esc}M}\right)^3 \quad (19)$$

The simulation of Schlichting et al. (2015) showed that if a 0.9  $M_{Earth}$  planet was hit by a Mars-sized impactor at a speed close to escape velocity, the corresponding atmospheric loss rate turned out to be 6%. Their results were 2 times lower than that calculated by Genda and Abe (2003), while the latter was based on a series assumption of the ground velocity.

## 6 The nonthermal escape processes

Since the Jeans escape and the hydrodynamic escape is highly related to the temperature of the upper atmosphere, typically both the two can be defined as a thermal escape. Nonthermal escape is a series of processes occurring as the velocity of escaping particles is not dominated by the upper atmospheric temperature. The nonthermal escape is the consequence of complex interactions including photochemical loss, ion pickup, sputtering, polar wind, etc.



### 6.1 Four common nonthermal escape mechanisms

Photochemical loss is similar to the Jeans escape except that the energetic particles are produced photochemically but not simply part of the tail of velocity distribution.

Ion pickup occurs mainly on the Sun-facing hemisphere of terrestrial planets where the solar wind impinges directly on the upper atmosphere. Ion pickup works mainly for planets without the protection of a strong magnetic field, such as Mars. Ions are created by photoionization, electron impact ionization and charge exchange during the interaction between the solar wind plasma and the upper atmosphere. Most of the pickup ions are accelerated efficiently and then escape to space.

Sputtering is another mechanism derived from ion pickup, it occurs when some pickup ions have sufficient energy to impart escape velocity to exospheric neutrals by collisions.

The polar wind is a process that a group of ions and plasma escape to space in the polar cap on a magnetized planet. The polar cap exists around the magnetic pole, where the magnetic field lines have one end in the ionosphere and the other in space. In the polar cap, the electrons are faster than the ions and thus set up an electric field accelerating ions upward, which leads to the occurrence of a polar wind.

According to Lammer (2012), as the hydrodynamically expanded thermosphere transfers into a hydrostatic regime with decreasing EUV, various non-thermal atmospheric escape processes start to become significant and contribute to the total atmospheric loss. During periods when the EUV flux of the young Sun decreased to values of  $\leq 7$  times that of the present, several non-thermal atmospheric escape processes, which might be less relevant during the first 500 Ma after the origin of the planets, began to act (Lammer 2012). However, the relevance of nonthermal escape related to proto-atmosphere can be much more complicated.

### 6.2 Minor roles nonthermal escape plays in atmospheric escape

Some authors suggested that the nonthermal escape mechanisms may not be significant during the early stage of the solar system. Kislyakova et al. (2013) studied the stellar wind-induced erosion of hydrogen upper atmosphere on an Earth-like planet in the habitable zone. They found that the loss rates of pickup  $H^+$  ions within a wide range of stellar wind plasma parameters are several times lower compared to the thermal escape rates. Johnson et al. (2013) pointed out that if the absorption of solar radiation energy in the upmost layer of the thermosphere is inefficient, nonthermal escape processes can be ignored. Tian (2013)

suggested the case in Johnson et al. (2013) can be considered as that the solar radiation energy absorbed in the collision-dominant part of the atmosphere contributes to the heating of the atmosphere but not to nonthermal escape processes. However, Airapetian et al. (2017) showed that non-thermal oxygen ion escape could be as important as the thermal hydrodynamic escape of hydrogen in removing the constituents of water from exoplanetary atmospheres under extreme high solar XUV irradiation. Moreover, the violent thermal escape especially as EUV-driven hydrodynamic escape could also contribute to some nonthermal escape processes.

### 6.3 The complicated relationship between the thermal and nonthermal escape

The magnetopause prevents the upper atmosphere from the erosion of solar plasma. The solar EUV flux from the young Sun can be extremely high thus the thermosphere can even expand beyond the magnetopause, meanwhile, the planetary gravity becomes weaker at higher exobase. In this case, nonthermal escape processes such as ion pickup would become relevant and contribute to the non-negligible mass-loss rate in atmospheric escape. Lichtenegger et al. (2010) investigated the Earth's exobase altitudes under different solar EUV fluxes. They found that the Earth's exobase level could move from the present location at about 500 km above the surface to about 2.4, 4.8, and 12.7  $R_{\text{Earth}}$  under solar EUV fluxes of 7 EUV, 10 EUV, and 20 EUV, respectively. Assuming that the Earth's intrinsic magnetic field could provide proto-atmosphere with effective protection from the solar wind, the extreme solar conditions make the Earth's magnetic field become too weak to protect the exosphere against strong ion pickup atmospheric escape processes. So far no numerical models have been established yet to provide accurate calculations on the atmospheric escape rates in this scenario.

Moreover, during nonthermal atmospheric escape processes, the interaction of the high-energy solar radiation and solar wind plasma with upper planetary atmospheres could modify the density and temperature profiles of the upper atmosphere. Therefore, the thermal and non-thermal atmospheric escape processes can be interrelated. However, there is still not a widely accepted nonthermal atmospheric escape model. This is because currently, we have a very limited understanding of the planetary magnetic field and solar wind's components from the young Sun, as well as the complicated interaction among non-thermal escape processes.

At present, it has been widely accepted that the early terrestrial planets are under intense stellar X-ray and EUV radiation so that the upper atmospheres on early terrestrial planets are necessarily hot. This makes the thermal escape,

especially hydrodynamic escape, the most inevitable atmospheric mass-loss mechanism when discussing the escape of proto-atmospheres.

## 7 Other research developments

As discussed in the previous section, atmospheric escape is a complex process because it is affected by many factors. We still need to gain a clearer knowledge about the dynamic mechanisms of proto-atmosphere escape on terrestrial planets. One might be wondering if there is a direct way to test the accuracy of different atmospheric models. Opposite to the models for the current atmospheres, there is much uncertainty for the proto-atmospheres. Vidal-Madjar et al. (2003) observed the atmosphere of an exoplanet named HD205498 through the detection of spectrum absorption. They found that the absorption area of atomic hydrogen was beyond the Roche limit, which refers to a fast escape event of hydrogen. Unfortunately, the current direct observation of atmospheric escape on exoplanets is mainly confined to close-in giant gas planets (i.e. giant gas planets orbiting near to their host star) including HD205498. So far no reliable observations of atmospheres on exo-terrestrial planets have been obtained (Gronoff et al. 2020; Owen et al. 2020), for which the current atmospheric escape models especially for hydrodynamic escape are mainly about gas giants. But better simulations can still provide us with some useful limitations on the possible scenarios of atmospheric evolution. Research developments in recent years are discussed below including an energy-limited multiple-components atmospheric escape model, the impacts of atmospheric escape on atmospheric chemistry, the impact-induced atmospheric erosion models, the combination of hydrodynamic escape, and impact erosion models.

### 7.1 An updated multiple-components hydrodynamic escape model

Guo (2019) studied the photoionization of H<sub>2</sub>O molecules in a dense steam atmosphere on an Earth-like planet that was exposed to EUV fluxes between 10 and 400 times the present solar values. It was shown that the H<sub>2</sub>O molecules dissociate and atomic H becomes the most abundant species around the 1 μ bar atmospheric level, while IR-cooling molecules such as CO<sub>2</sub> could not reach this altitude due to mass fractionation. This work provides further proof of a hydrogen-dominated upper atmosphere and a clearer lower boundary of EUV-driven energy-limited hydrodynamic escape region. Odert et al. (2018) proposed a three-components proto-atmosphere model based on the method of Zahnle and Kasting (1986) and Zahnle et al. (1990). They

suggested that the H<sub>2</sub>O–CO<sub>2</sub> proto-atmospheres can be lost in a few up to a few tens of Ma from Mars. However, the start time of atmospheric escape they assumed, 10 Ma of solar age, seems too early and may affect the preservation of proto-atmospheres significantly. Benedikt et al. (2020) followed this work and further developed a multiple-components atmosphere model. They took 1 μbar as the lower boundary of the hydrodynamic escape region and concluded that for all simulated cases the entire budget of outgassed moderately volatile elements and noble gases from the magma ocean is lost due to hydrodynamic escape as long as the embryo is located within about 2 AU.

### 7.2 The effect of atmospheric escape on atmospheric chemistry

The hydrodynamically escaping hydrogen atoms preferentially drag the lighter isotopes and thus the proto-atmosphere tends to accumulate heavier isotopes. Meanwhile, the major heavy species can drag the minor heavier ones as well. The present Martian CO<sub>2</sub>-dominated atmosphere actually prevents the expansion of the upper atmosphere, which further prevents the occurrence of hydrodynamic escape. Therefore the loss of Mars' atmospheric nitrogen must have happened at an early stage. According to the estimated amount of the lost nitrogen based on the structure and composition data from MAVEN, the surface pressure of Mars was most likely higher than 0.5 bar about 4 Ga ago (Kurokawa et al. 2018). The thermodynamic model applied by Chevrier et al. (2007) indicated that the estimated high oxidation state of the early Martian surface supports an efficient escape of hydrogen. Besides, the enrichment of <sup>15</sup>N in the atmosphere of Mars indicates that Mars has lost most of its atmospheric nitrogen inventory (Füri and Marty 2015).

Noble gases are relatively useful to constrain the atmospheric evolution since they are mostly partitioned into the atmosphere and do not form molecules to participate in most reactions. Pepin (1997) suggested that hydrodynamic escape on early Venus could generate Ne and Ar isotope ratios which are close to the observed values in its present atmosphere. However, the isotope fractionation caused by hydrodynamic escape may not be significant. Benedikt et al. (2020) investigated the hydrodynamic escape of noble gas on planetary embryos with mass less than 1.5 M<sub>Mars</sub>. In these cases, they found that due to the high mass-loss rate, the initial fractionations of <sup>20</sup>Ne/<sup>22</sup>Ne and <sup>36</sup>Ar/<sup>38</sup>Ar could not change significantly, even for a proto-atmosphere that has lost most of its noble gases. Lammer et al. (2021) investigated that there is a reasonable mass range for the proto-Earth and proto-Venus depending on their <sup>36</sup>Ar/<sup>38</sup>Ar and <sup>20</sup>Ne/<sup>22</sup>Ne. Below this range, there would not be enough <sup>36</sup>Ar and <sup>20</sup>Ne to lose,

and beyond this range, there would be too many lighter isotopes to get rid of.

### 7.3 The impact-induced atmospheric erosion models

Except for the solar EUV, impact events can also contribute to the hydrodynamic escape. According to Schlichting et al. (2015), the atmospheric mass-loss caused by hydrodynamic escape due to the high surface temperature induced by giant impacts could be significantly higher than the atmospheric erosion caused by the global earthquake (Schlichting et al. 2015; Inamdar and Schlichting 2015, 2016).

Shuvalov (2009) first developed a two-dimension model to simulate oblique impacts participated by small impactors. They found that the local atmospheric escape increased as the frequency of small impactors increased, which shows a reverse trend to giant impacts. Although 1-2D models can calculate the effect of ground velocity on atmospheric escape, these models ignored the significant deformation of both ground and atmosphere caused by impacts. Liu et al. (2015) simulated the consequences of impact events on the super-Earths and found that the giant impact can remove most of the H/He primordial atmosphere immediately. Hwang et al. (2018) modeled the large-angle impact events, mainly focusing on the interrelation between impactors and the atmosphere. Both Liu et al. (2015) and Hwang et al. (2018) developed three-dimension models but assumed dense atmospheres. In order to reproduce the impact erosion in the early solar system, we need to focus on thinner atmospheric structure and more realistic impact erosion systems. Kegerreis et al. (2020) suggested that atmospheric mass loss induced by head-on impacts change more significantly than that of grazing impacts with different initial parameters.

### 7.4 The combination of hydrodynamic escape and impact erosion models

Hydrodynamic escape and atmospheric impact erosion processes are two violent escape processes experienced by the original atmospheres of terrestrial planets. Although neither of them can cause significant isotope fractionation independently, the combination of both could lead to more realistic simulations of the proto-atmospheres on terrestrial planets. By assuming that the proto-Earth had accumulated to more than  $0.5 M_{\text{Earth}}$  before the nebula disk dissipated, Lammer et al. (2020) combined the simulation results of hydrodynamic escape with that of impact erosion, successfully recovering the composition of  $^{36}\text{Ar}/^{38}\text{Ar}$  and  $^{20}\text{Ne}/^{22}\text{Ne}$  in the present atmosphere. Moreover, according

to Biersteker and Schlichting (2019), the atmospheric mass-loss rate in hydrodynamic escape due to the high surface temperature caused by giant impacts can be significantly higher than the atmospheric erosion caused by the global earthquake (Schlichting et al. 2015; Inamdar and Schlichting 2015, 2016).

### 7.5 The influence of planetary magnetic field on atmospheric escape

Magnetospheres exist both around magnetized planets, such as Earth, and unmagnetized planets, such as Venus and Mars. At a magnetized planet, the magnetosphere is the part of space dominated by the planetary magnetic field, and the magnetopause is the outer boundary of the magnetosphere. Around an unmagnetized planet with an atmosphere, an induced magnetosphere can be formed by the interaction between the upper atmosphere and the solar wind (Russell 1993). Its outer boundary is called the induced magnetosphere boundary (Lundin et al. 2004). The induced magnetosphere boundary is located closer to the planet than the magnetopause is to a magnetized planet.

To what extent the presence or absence of a magnetic field around a planet influence the atmospheric escape is a controversial issue. It has been suggested that magnetized planets are better protected against atmospheric loss (Kulikovic et al. 2007; Dehant et al. 2007) because an intrinsic magnetosphere could provide direct shielding of the atmosphere by deflecting solar wind away from the planet. The Earth's atmosphere without a magnetic field is believed to be escaping more efficiently (Gronoff et al. 2020).

However, some researches showed that an intrinsic magnetic field does not necessarily protect a planet from losing its atmosphere (Brain et al. 2013; Garcia-Sage et al. 2017; Gunell et al. 2018).

The magnetosphere around a planet diverts part of the solar wind energy and protects the atmosphere from sputtering and ion pickup. The induced magnetospheres of the unmagnetized planets also provide protection from sputtering and ion pickup but to a lesser extent. However, Brain et al. (2013) suggested that the amount of energy transferred from the stellar wind to the ionosphere of a magnetized planet is not necessarily lower for unmagnetized planets. Garcia-Sage et al. (2017) investigated an exoplanet called Proxima b, which orbits at the location where an Earth would not freeze or boil its oceans. The simulation showed that even in the case of an Earth-like intrinsic magnetic field, the evolution of the atmosphere of Proxima b would be very different from that of the Earth.

Gunell et al. (2018) calculated the total mass-loss rate including several nonthermal escape processes that depend on the planetary magnetic moment in the present solar system. The authors found that while a planetary magnetic field protects the atmosphere from sputtering and ion pickup, it contributes to other atmospheric escape processes around the polar cap, such as polar wind, which further increases the escape rate.

## 8 Discussion and summary

Here we have reviewed the formation and evolution of the proto-atmosphere, and concluded three major atmospheric escape mechanisms: boil-off, hydrodynamic escape, impact erosion. We also introduce some other atmospheric escape mechanisms including Jeans escape and nonthermal escape.

The “boil-off” occurs during the nebula disk dissipation, it is a short-term but violent escape mechanism, crucial for whether or not the nebula material could be captured by proto-atmospheres. Basically, “boil-off” refers to an atmospheric escape process that is similar to boiling and occurs during the rapid decrease of nebula disk pressure. “Boil-off” could cause a large part of primordial atmosphere loss to space. Due to its complexity, very limited numerical models on “boil-off” have been established, the established ones still remain controversial issues (Owen and Wu 2016; Fossati et al. 2017; Kubyshkina et al. 2018). On one hand, “boil-off” is strictly controlled by how fast the nebula disk dissipated. If the nebula disk dissipated slowly, “boil-off” may not even exist, whereas the timescale of nebula disk dispersal still remains unclear. On the other hand, the dynamic mechanism of “boil-off” is very complicated. A large number of free surfaces could be produced during this process, which means the traditional CFD method becomes inaccurate to describe it. Thus a more appropriate model is needed. Moreover, the present models are limited on the planets  $\geq 3 M_{\text{Earth}}$ , and we need to further expand this mass scale to a lower boundary.

Compared to the “boil-off”, hydrodynamic escape is a relatively long-term atmospheric mass-loss process. Since the hydrodynamic escape also corresponds to a high mass-loss rate, it is considered the most important atmospheric escape mechanism for proto-atmospheres. The dynamic models related to hydrodynamic escape have been well established, especially for the ones based on energy-limited theory. So far the energy-limited hydrodynamic escape models are capable of calculating the mass-loss rate for multi-component atmospheres, but the accuracy can still be further optimized: (1) Some parameters still remain in assumption. For example, there is still not an accurate value for solar heating efficiency  $\eta$  for terrestrial planets,

which can lead to non-negligible variations on the atmospheric mass-loss rate. (2) The structure of proto-atmosphere is divided into the lower atmosphere and the upper atmosphere. Only the upper atmosphere is heated efficiently by solar EUV and experiences hydrodynamic escape, meanwhile, the materials are transferred by diffusion from the lower to the upper atmosphere. If the mass-loss rate of the upper atmosphere goes too high, this diffusion process could provide an upper limit for the upper atmospheric mass-loss rate, which needs to be further evaluated. (3) There is a huge variation of atmospheric physical and chemical parameters, such as density and components, from the planetary surface to the outer boundary of proto-atmosphere. The variation of these parameters could influence the atmospheric escape rate as well. However, most of the current atmospheric models remain in one dimension, which decreases the reliability of calculations. Thus more accurate atmospheric models need to be established.

There is no doubt that the impact events can cause significant atmospheric erosion, but the impact events both contribute to the supply and loss of atmospheric materials, especially for small impactors. As the small impactors travel through the atmosphere, they are rubbed violently by the dense atmosphere as well, during which a large amount of volatiles are released and then remain in the proto-atmosphere. Because the proto-atmosphere can be hundreds of times denser than the present atmosphere, the friction can be so violent that most the volatiles can be released into the atmosphere for small or even large impactors. We have not yet established an accurate model to evaluate this volatile delivery mechanism. Another problem for investigating the impact events is that we have limited knowledge on the impact events histories, such as the mass, velocity, and time distribution of impactors, which is crucial to further simulate the influence of impact events on the evolution of proto-atmosphere. Moreover, although many impact erosion models have been established for different scales of impactors, the inevitable assumptions have limited the accuracy of these models. In conclusion, the development of impact-induced atmospheric escape models is still in a primary stage, many fundamental issues are still needed to get solved.

So far there is still not an accurate model to simulate the nonthermal atmospheric escape mechanisms for proto-atmospheres. Some groups used the nonthermal atmospheric escape models for present solar systems to evaluate the mass-loss rate of proto-atmosphere in the early solar system. They suggested that the mass-loss rate of nonthermal escape can be negligible compared to the thermal escape especially the hydrodynamic escape, while some other authors suggested the mass-loss rate of the two can be comparable. This controversial issue exists because the

lack of knowledge about the solar wind and plasma environment prevents us from establishing a comprehensive nonthermal escape model for terrestrial proto-atmospheres.

The mechanisms mentioned above are interrelated because they could be existing simultaneously. Some authors have investigated the contribution of impact-induced planetary surface heating to the hydrodynamic escape. A few models have been established to simulate the transition from hydrodynamic escape to Jeans escape. However, some other processes need to be further investigated as well, such as the transition from “boil-off” to hydrodynamic escape, the influence of hydrodynamic atmospheric expansion on the nonthermal escape.

The atmospheric escape mechanisms were often considered separately in most cases, therefore in the future, we need to develop more comprehensive models to establish a better understanding of the escape scenarios of proto-atmospheres. Geochemistry ratios and atmospheric models are also tending to get combined deeper to provide us with more reasonable calculations.

**Acknowledgements** This research was jointly supported by National Science Foundation (41973063), Strategic Priority Research Program (B) of CAS (XDB18010100, XDB41000000), Pre-research Project of Civil Aerospace Technologies (D020202), and Chinese National Space Administration and Chinese NSF Projects (41903019, 41530210).

#### Declarations

**Conflict of interest** On behalf of all authors, the corresponding author states that there is no conflict of interest.

**Ethical standards** This paper compliance with Ethical Standards. We declare that we have no financial and personal relationships with other people or organizations that can inappropriately influence our work, there is no professional or other personal interest of any nature or kind in any product, service and/or company that could be construed as influencing the position presented in, or the review of, the manuscript entitled.

#### References

- Ahrens TJ (1993) Impact erosion of terrestrial planetary atmospheres. *Annu Rev Earth Planet Sci* 21(1):525–555
- Airapetian VS, Glocer A, Khazanov GV, Loyd ROP, France K, Sojka J, Danchi WC, Liemohn MW (2017) How hospitable are space weather affected habitable zones? The role of ion escape. *Astrophys J Lett* 836(1):L3
- Benedikt MR, Scherf M, Lammer H, Marcq E, Odert P, Leitzinger M, Erkaev NV (2020) Escape of rock-forming volatile elements and noble gases from planetary embryos. *Icarus* 347:113772
- Brain DA, Leblanc F, Luhmann JG, Moore TE, Tian F (2013) Planetary magnetic fields and climate evolution. *Comp Climatol Terr Planets* 487
- Catling DC (2006) Comment on “A hydrogen-rich early Earth atmosphere”. *Science (New York, N.Y.)* 311(5757):38
- Chamberlain JW (1963) Planetary coronae and atmospheric evaporation. *Planet Space Sci* 11(8):901–960
- Chassefière E (1996) Hydrodynamic escape of hydrogen from a hot water-rich atmosphere: the case of Venus. *J Geophys Res Planets* 101(E11):26039–26056
- Chen GQ, Ahrens TJ (1997) Erosion of terrestrial planet atmosphere by surface motion after a large impact. *Phys Earth Planet Inter* 100(1–4):21–26
- Chevrier V, Poulet F, Bibring JP (2007) Early geochemical environment of Mars as determined from thermodynamics of phyllosilicates. *Nature* 448(7149):60–63
- Dehant V, Lammer H, Kulikov YN, Grießmeier JM, Breuer D, Verhoeven O, Karatekin Ö, Van Hoolst T, Korablev O, Lognonné P (2007) Planetary magnetic dynamo effect on atmospheric protection of early Earth and Mars. *Space Sci Rev* 129(1–3):279–300
- Edgar R (2004) A review of Bondi–Hoyle–Lyttleton accretion. *New Astron Rev* 48(10):843–859
- Elkins-Tanton LT (2008) Linked magma ocean solidification and atmospheric growth for Earth and Mars. *Earth Planet Sci Lett* 271(1–4):181–191
- Elkins-Tanton LT (2011) Formation of early water oceans on rocky planets. *Astrophys Space Sci* 332(2):359–364
- Erkaev NV, Kulikov YN, Lammer H, Selsis F, Langmayr D, Jaritz GF, Biernat HK (2007) Roche lobe effects on the atmospheric loss from “Hot Jupiters.” *Astron Astrophys* 472(1):329–334
- Erkaev NV, Lammer H, Elkins-Tanton LT, Stökl A, Odert P, Marcq E, Dorfi EA, Kislyakova KG, Kulikov YuN, Leitzinger M, Güdel M (2014) Escape of the martian protoatmosphere and initial water inventory. *Planet Space Sci* 98:106–119
- Erkaev NV, Lammer H, Odert P, Kulikov YN, Kislyakova KG (2015) Extreme hydrodynamic atmospheric loss near the critical thermal escape regime. *Mon Not R Astron Soc* 448(2):1916–1921
- Erkaev NV, Lammer H, Odert P, Kulikov YN, Kislyakova KG, Khodachenko ML, Güdel M, Hanslmeier A, Biernat H (2013) XUV-exposed, non-hydrostatic hydrogen-rich upper atmospheres of terrestrial planets. Part I: atmospheric expansion and thermal escape. *Astrobiology* 13(11):1011–1029
- Fossati L, Erkaev NV, Lammer H et al (2017) Aeronomical constraints to the minimum mass and maximum radius of hot low-mass planets. *Astron Astrophys* 598:A90
- Füri E, Marty B (2015) Nitrogen isotope variations in the Solar System. *Nat Geosci* 8(7):515–522
- Garcia-Sage K, Glocer A, Drake JJ, Gronoff G, Cohen O (2017) On the magnetic protection of the atmosphere of Proxima Centauri b. *Astrophys J Lett* 844(1):L13
- Genda H, Abe Y (2003) Survival of a proto-atmosphere through the stage of giant impacts: the mechanical aspects. *Icarus* 164(1):149–162
- Genda H, Abe Y (2005) Enhanced atmospheric loss on protoplanets at the giant impact phase in the presence of oceans. *Nature* 433(7028):842–844
- Ginzburg S, Schlichting HE, Sari RE (2016) Super-Earth atmospheres: self-consistent gas accretion and retention. *Astrophys J* 825(1):29
- Gomes R, Levison HF, Tsiganis K, Morbidelli A (2005) Origin of the cataclysmic Late Heavy Bombardment period of the terrestrial planets. *Nature* 435(7041):466–469
- Gorti U, Hollenbach D, Dullemond CP (2015) The impact of dust evolution and photoevaporation on disk dispersal. *Astrophys J* 804(1):29
- Gronoff G, Arras P, Baraka S, Bell JM, Cessateur G, Cohen O, Drake JJ, Elrod M, Erwin J, Garcia-Sage K, Garraffo C, Glocer A, Heavens NG, Lovato K, Maggiolo R, Parkinson CD, Simon Wedlund C, Weimer DR, Moore WB (2020) Atmospheric escape processes and planetary atmospheric evolution. *J Geophys Res: Space Phys* 125(8):e2019JA027639

- Gunell H, Maggiolo R, Nilsson H, Wieser GS, Slapak R, Lindkvist J, Hamrin M, De Keyser J (2018) Why an intrinsic magnetic field does not protect a planet against atmospheric escape. *Astron Astrophys* 614:L3
- Guo JH (2019) The effect of photoionization on the loss of water of the planet. *Astrophys J* 872(1):99
- Hamano K, Abe Y, Genda H (2013) Emergence of two types of terrestrial planet on solidification of magma ocean. *Nature* 497(7451):607–610
- Hunten DM (1982). Thermal and nonthermal escape mechanisms for terrestrial bodies. *Planet Space Sci* 30(8):773–783. [https://doi.org/10.1016/0032-0633\(82\)90110-6](https://doi.org/10.1016/0032-0633(82)90110-6)
- Hwang J, Chatterjee S, Lombardi J Jr, Steffen JH, Rasio F (2018) Outcomes of Grazing Impacts between Sub-Neptunes in Kepler Multis. *Astrophys J* 852(1):41
- Ikoma M, Genda H (2006) Constraints on the mass of a habitable planet with water of nebular origin. *Astrophys J* 648(1):696
- Ikoma M, Hori Y (2012) In situ accretion of hydrogen-rich atmospheres on short-period super-Earths: implications for the Kepler-11 planets. *Astrophys J* 753(1):66
- Ikoma M, Nakazawa K, Emori H (2000) Formation of giant planets: dependences on core accretion rate and grain opacity. *Astrophys J* 537(2):1013
- Inamdar NK, Schlichting HE (2015) The formation of super-Earths and mini-Neptunes with giant impacts. *Mon Not R Astron Soc* 448(2):1751–1760
- Inamdar NK, Schlichting HE (2016) Stealing the gas: giant impacts and the large diversity in exoplanet densities. *Astrophys J Lett* 817(2):L13
- John B, Biersteker Hilke E, Schlichting (2019) Atmospheric mass-loss due to giant impacts: the importance of the thermal component for hydrogen–helium envelopes. *Monthly Notices of the Royal Astronomical Society* 485(3):4454–4463. <https://doi.org/10.1093/mnras/stz738>
- Johnson RE, Volkov AN, Erwin JT (2013) Molecular-kinetic simulations of escape from the ex-planet and exoplanets: criterion for transonic flow. *Astrophys J Lett* 768(1):L4
- Johnstone CP, Güdel M, Stökl A, Lammer H, Tu L, Kislyakova KG, Lüftinger T, Odert P, Erkaev NV, Dorfi EA (2015) The evolution of stellar rotation and the hydrogen atmospheres of habitable-zone terrestrial planets. *Astrophys J Lett* 815(1):L12
- Kasting JF, Pollack JB (1983) Loss of water from Venus. I. Hydrodynamic escape of Hydrogen. *Icarus* 53(3):479–508
- Kegerreis JA, Eke VR, Massey RJ, Teodoro LFA (2020) Atmospheric erosion by giant impacts onto terrestrial planets. *Astrophys J* 897(2):161
- Kislyakova KG, Lammer H, Holmström M, Panchenko M, Odert P, Erkaev NV, Leitzinger M, Khodachenko ML, Kulikov YN, Güdel M, Hanslmeier A (2013) XUV-exposed, non-hydrostatic hydrogen-rich upper atmospheres of terrestrial planets. Part II: hydrogen coronae and ion escape. *Astrobiology* 13(11):1030–1048
- Koskinen TT, Yelle RV, Lavvas P, Lewis NK (2010) Characterizing the thermosphere of HD209458b with UV transit observations. *Astrophys J* 723(1):116
- Kubyskhina D, Fossati L, Erkaev NV, Johnstone CP, Cubillos PE, Kislyakova KG, Lammer H, Lendl M, Odert P (2018) Grid of upper atmosphere models for 1–40  $M_{\oplus}$  planets: application to CoRoT-7 b and HD 219134 b, c. *Astron Astrophys* 619:A151
- Kulikov YN, Lammer H, Lichtenegger HI, Penz T, Breuer D, Spohn T, Lundin R, Biernat HK (2007) A comparative study of the influence of the active young Sun on the early atmospheres of Earth, Venus, and Mars. *Space Sci Rev* 129(1–3):207–243
- Lammer H, Kasting JF, Chassefière E, Johnson RE, Kulikov YN, Tian F (2008). Atmospheric escape and evolution of terrestrial planets and satellites. *Space Sci Rev* 139(1–4):399–436
- Kurokawa H, Kurosawa K, Usui T (2018) A lower limit of atmospheric pressure on early Mars inferred from nitrogen and argon isotopic compositions. *Icarus* 299:443–459
- Lammer H, Blanc M (2018) From disks to planets: the making of planets and their early atmospheres. *An Introduction Space Science Reviews* 214(2):1–35
- Lammer H, Chassefière E, Karatekin Ö, Morschhauser A, Niles PB, Mousis O, Odert P, Möstl UV, Breuer D, Dehant V, Grott M, Gröller H, Hauber E (2013) Outgassing history and escape of the Martian atmosphere and water inventory. *Space Sci Rev* 174(1):113–154
- Lammer H, Zerkle AL, Gebauer S, Tosi N, Noack L, Scherf M, Pilat-Lohinger E, Güdel M, Grenfell JL, Godolt M, Nikolaou A (2018) Origin and evolution of the atmospheres of early Venus, Earth and Mars. *Astron Astrophys Rev* 26(1):1–72
- Lammer H, Brassler R, Johansen A, Scherf M, Leitzinger M (2021) Formation of Venus, Earth and Mars: constrained by isotopes. *Space Sci Rev* 217(1):1–35
- Lammer H, Erkaev NV, Odert P, Kulikov YN, Kislyakova KG, Stoekl A, Dorfi EA, Güdel M, Leitzinger M (2014) Loss of nebula-captured hydrogen envelopes from ‘sub’-to ‘super-Earths’ in the habitable zone of Sun-like stars. In EGU general assembly conference abstracts (p 13276)
- Lammer H, Leitzinger M, Scherf M, Odert P, Burger C, Kubyskhina D, Johnstone C, Maindl T, Schäfer CM, Güdel M, Tosi N, Nikolaou A, Marcq E, Erkaev NV, Noack L, Kislyakova KG, Fossati L, Pilat-Lohinger E, Ragossnig F, Dorfi EA (2020) Constraining the early evolution of Venus and Earth through atmospheric Ar, Ne isotope and bulk K/U ratios. *Icarus* 339:113551
- Lammer H (2012) Origin and evolution of planetary atmospheres: implications for habitability Springer Science & Business Media
- Lebrun T, Massol H, Chassefière E, Davaille A, Marcq E, Sarda P, Leblanc F, Brandeis G (2013) Thermal evolution of an early magma ocean in interaction with the atmosphere. *J Geophys Res: Planets* 118(6):1155–1176
- Lichtenegger HIM, Lammer H, Grießmeier JM, Kulikov YN, von Paris P, Hausleitner W, Krauss S, Rauer H (2010) Aeronomical evidence for higher CO<sub>2</sub> levels during Earth’s Hadean epoch. *Icarus* 210(1):1–7
- Liu SF, Hori Y, Lin DNC, Asphaug E (2015) Giant impact: an efficient mechanism for the devolatilization of super-Earths. *Astrophys J* 812(2):164
- Luger R, Barnes R, Lopez E, Fortney J, Jackson B, Meadows V (2015) Habitable evaporated cores: transforming mini-Neptunes into super-Earths in the habitable zones of M dwarfs. *Astrobiology* 15(1):57–88
- Lundin R, Barabash S, Andersson H, Holmström M, Grigoriev A, Yamauchi M, Sauvaud J-A, Fedorov A, Budnik E, Thocaven J-J, Wingham D, Frahm R, Scherrer J, Sharber J, Asamura K, Hayakawa H, Coates A, Linder DR, Curtis C, Hsieh KC, Sandel BR, Grande M, Carter M, Reading DH, Koskinen H, Kallio E, Riihela P, Schmidt W, Säles T, Kozyra J, Krupp N, Woch J, Luhmann J, McKenna-Lawler S, Cerulli-Irelli R, Orsini S, Maggi M, Mura A, Milillo A, Roelof E, Williams E, Livi S, Brandt P, Wurz P, Bochsler P (2004) Solar wind-induced atmospheric erosion at Mars: first results from ASPERA-3 on Mars Express. *Science* 305(5692):1933–1936
- Marcq E (2012) A simple 1-D radiative-convective atmospheric model designed for integration into coupled models of magma ocean planets. *J Geophys Res: Planets* 117(E1)
- Massol H, Hamano K, Tian F, Ikoma M, Abe Y, Chassefière E, Davaille A, Genda H, Güdel M, Hori Y, Leblanc F, Marcq E, Sarda P, Shematovich VI, Stökl A, Lammer H (2016) Formation and evolution of protoatmospheres. *Space Sci Rev* 205(1):153–211

- Melosh HJ, Vickery AM (1989) Impact erosion of the primordial atmosphere of Mars. *Nature* 338(6215):487–489
- Mizuno H, Nakazawa K, Hayashi C (1978) Instability of a gaseous envelope surrounding a planetary core and formation of giant planets. *Progress Theoret Phys* 60(3):699–710
- Morbidelli A, Nesvorný D, Laurenz V, Marchi S, Rubie DC, Elkins-Tanton L, Wieczorek M, Jacobson S (2018) The timeline of the lunar bombardment: revisited. *Icarus* 305:262–276
- Murray-Clay RA, Chiang EI, Murray N (2009) Atmospheric escape from hot Jupiters. *Astrophys J* 693(1):23
- Odert P, Lammer H, Erkaev NV, Nikolaou A, Lichtenegger HI, Johnstone CP, Kislyakova KG, Leitzinger M, Tosi N (2018) Escape and fractionation of volatiles and noble gases from Mars-sized planetary embryos and growing protoplanets. *Icarus* 307:327–346
- Öpik EJ (1963) Selective escape of gases. *Geophys J Int* 7(4):490–509
- Owen JE, Jackson AP (2012) Planetary evaporation by UV and X-ray radiation: basic hydrodynamics. *Mon Not R Astron Soc* 425(4):2931–2947
- Owen JE, Wu Y (2016) Atmospheres of low-mass planets: the “boil-off.” *Astrophys J* 817(2):107
- Owen JE, Shaikhislamov IF, Lammer H, Fossati L, Khodachenko ML (2020) Hydrogen dominated atmospheres on terrestrial mass planets: evidence, origin and evolution. *Space Sci Rev* 216(8):1–24
- Parker EN (1964) Dynamical properties of Stellar Coronas and Stellar Winds. I. Integration of the momentum equation. *Astrophys J* 139:72
- Penz T, Erkaev NV, Kulikov YN, Langmayr D, Lammer H, Micela G, Cecchi-Pestellini C, Biernat HK, Selsis F, Barge P, Deleuil M, Léger A (2008) Mass loss from “Hot Jupiters”—Implications for CoRoT discoveries, Part II: long time thermal atmospheric evaporation modeling. *Planet Space Sci* 56(9):1260–1272
- Pepin RO (1997) Evolution of Earth’s noble gases: consequences of assuming hydrodynamic loss driven by giant impact. *Icarus* 126(1):148–156
- Ribas I, Guinan EF, Güdel M, Audard M (2005) Evolution of the solar activity over time and effects on planetary atmospheres. I. High-energy irradiances (1–1700 Å). *Astrophys J* 622(1):680
- Russell CT (1993) Planetary magnetospheres. *Rep Prog Phys* 56(6):687
- Salvador A, Massol H, Davaille A, Marcq E, Sarda P, Chassefière E (2017) The relative influence of H<sub>2</sub>O and CO<sub>2</sub> on the primitive surface conditions and evolution of rocky planets. *J Geophys Res: Planets* 122(7):1458–1486
- Schlichting HE, Mukhopadhyay S (2018) Atmosphere impact losses. *Space Sci Rev* 214(1):1–31
- Schlichting HE, Sari RE, Yalinewich A (2015) Atmospheric mass loss during planet formation: the importance of planetesimal impacts. *Icarus* 247:81–94
- Shuvalov V (2009) Atmospheric erosion induced by oblique impacts. *Meteorit Planet Sci* 44(8):1095–1105
- Spitzer L Jr (1952) Equations of Motion for an Ideal Plasma. *Astrophys J* 116:299
- Stökl A, Dorfi EA, Johnstone CP, Lammer H (2016) Dynamical accretion of primordial atmospheres around planets with masses between 0.1 and 5 M<sub>⊕</sub> in the habitable zone. *Astrophys J* 825(2):86
- Tian F (2013) Conservation of total escape from hydrodynamic planetary atmospheres. *Earth Planet Sci Lett* 379:104–107
- Tian F, Toon OB, Pavlov AA, De Sterck H (2005) A hydrogen-rich early Earth atmosphere. *Science* 308(5724):1014–1017
- Tian F, Toon OB, Pavlov AA (2006) Response to comment on “A hydrogen-rich early Earth atmosphere”. *Science* 311(5757):38–38
- Tian F, Güdel M, Johnstone CP, Lammer H, Luger R, Odert P (2018) Water loss from young planets. *Space Sci Rev* 214(3):1–19
- Tian F, Kasting JF, Liu HL, Roble RG (2008) Hydrodynamic planetary thermosphere model: 1. Response of the Earth’s thermosphere to extreme solar EUV conditions and the significance of adiabatic cooling. *J Geophys Res: Planets* 113(E5)
- Tu L, Johnstone CP, Güdel M, Lammer H (2015). The extreme ultraviolet and X-ray Sun in Time: High-energy evolutionary tracks of a solar-like star. *Astron Astrophys* 577, L3.
- Vickery AM, Melosh HJ (1990) Atmospheric erosion and impactor retention in large impacts, with application to mass extinctions. *Global Catastrophes in Earth History* 247:289–300
- Vidal-Madjar A, Des Etangs AL, Désert JM, Ballester GE, Ferlet R, Hébrard G, Mayor M (2003) An extended upper atmosphere around the extrasolar planet HD209458b. *Nature* 422(6928):143–146
- Watson AJ, Donahue TM, Walker JC (1981) The dynamics of a rapidly escaping atmosphere: applications to the evolution of Earth and Venus. *Icarus* 48(2):150–166
- Wuchterl G (1993) The critical mass for protoplanets revisited: massive envelopes through convection. *Icarus* 106(1):323–334
- Xie M, Xiao Z, Xu L, Fa W, Xu A (2021) Change in the Earth–Moon impactor population at about 3.5 billion years ago. *Nature Astronomy* 5(2):128–133
- Yelle RV (2004) Aeronomy of extra-solar giant planets at small orbital distances. *Icarus* 170(1):167–179
- Young ED, Shahar A, Nimmo F, Schlichting HE, Schauble EA, Tang H, Labidi J (2019) Near-equilibrium isotope fractionation during planetesimal evaporation. *Icarus* 323:1–15
- Zahnle KJ, Kasting JF (1986) Mass fractionation during transonic escape and implications for loss of water from Mars and Venus. *Icarus* 68(3):462–480
- Zahnle K, Kasting JF, Pollack JB (1990) Mass fractionation of noble gases in diffusion-limited hydrodynamic hydrogen escape. *Icarus* 84(2):502–527
- Zel’dovich YB, Raizer YP (1967) *Physics of shock waves and high-temperature hydrodynamic phenomena*. Academic, New York